PHOTONICS Research

# Polymer waveguide tunable transceiver for photonic front-end in the 5G wireless network

Tae-Hyun Park, Sung-Moon Kim, Eun-Su Lee, and Min-Cheol Oh*

*Department of Electronics Engineering, Pusan National University, Pusan (Busan) 46241, Republic of Korea*
**Corresponding author: mincheoloh@pusan.ac.kr*

*Received 29 September 2020; revised 23 November 2020; accepted 7 December 2020; posted 8 December 2020 (Doc. ID 411137); published 26 January 2021*

**A photonic front-end in the 5G wireless network based on wavelength-division multiplexing optical communication requires low-cost tunable transceivers. By exploiting polymer waveguide Bragg-grating technology, we propose a tunable transceiver consisting of an external cavity tunable laser and a tilted grating tunable filter. In particular, a double-reflection tunable filter provides narrower reflection bandwidth and suppresses undesired mode coupling, improving the side-mode suppression ratio (SMSR) and reducing adjacent-channel crosstalk. By introducing perfluorinated polymers with low birefringence, polarization independence, which is a prerequisite for wavelength filter elements, is secured, and 20 dB bandwidth of 0.69 nm, wavelength tunability over 40 nm, and SMSR of 42 dB are achieved.** © 2021 Chinese Laser Press

https://doi.org/10.1364/PRJ.411137

## 1. INTRODUCTION

The recent explosive expansion of web-based video platform services has been unceasingly increasing data traffic and has become a driving force in the development of next-generation communication technologies. Wavelength-division-multiplexed (WDM) optical communication technology, which provides advantages such as high bandwidth, protocol transparency, and scalability, has become an important technology not only in metro-core networks but also in the fronthauls connecting radio-access networks [1,2]. Unlike core networks, fronthaul WDM networks require cost-effective network equipment, for which low-cost WDM transceivers are crucial [3]. Currently, the WDM system for the 5G fronthaul is set to meet the transmission distance of 10 km by using 10 Gbit/s transmission rate, 100 GHz channel spacing, and 48 wavelength channels in the C, L, and O bands. For this purpose, tunable laser technology has matured, while tunable filters are not yet available, making it difficult to find inexpensive tunable transceivers. By developing an integrated optic tunable filter with high performance, an integrated tunable transceiver could be realized to reduce the burden for deploying tunable wavelength transceivers for 5G fronthaul networks.

To provide the light sources of various wavelengths for WDM, a tunable laser with low inventory burden and low price is an attractive option [4–8]. The tunable laser in charge of each channel is set to operate at different wavelengths and is modulated using the information to be transmitted. The multiplexed wavelength signals arriving at the receiving end are demultiplexed using a thin-film filter or an arrayed waveguide grating (AWG). In early WDM optical communication systems with a small number of wavelength channels, thin-film filters were mainly used because of the simplicity and high production yield [9]. As the number of wavelength channels increased, AWG became more suitable for demultiplexing a large number of wavelength channels. However, the AWG separates each wavelength into a different fiber, so if the transmitter wavelength changes, the fiber must be reconfigured manually [10]. In contrast, with a tunable wavelength filter, the receiver can adjust the filtering wavelength simultaneously without manually switching the fiber.

Various approaches for implementing tunable filters include micro-electromechanical system-based Fabry–Perot (FP) filters, FP devices using the electroclinic effect of liquid crystals, acousto-optic filters using mode coupling, fiber Bragg gratings with piezoelectric actuators, and ring resonators with thermal tuning [11–16]. However, the above devices are not suitable for laser integration to produce compact tunable transceivers. In this work, we propose a polymeric optical waveguide tunable transceiver enabling the integration of a tunable laser and a tunable filter on a single chip. Both polymer lasers and filters include Bragg gratings with different structures, and they are fabricated simultaneously through a compatible fabrication process. Because the polymer has high thermo-optic (TO) effect and strong thermal confinement, wide tuning of Bragg wavelength is available, and because of the simple device structure, wavelength control is easy and high production yield is achievable [17].

In order to demonstrate a high-performance tunable filter device for WDM systems, we have been working on various

approaches. Apodized Bragg gratings fabricated using shadow masks were effective in reducing the reflection bandwidth and improving the side-mode suppression ratio (SMSR) [18]. Asymmetric Y-branches and tilted Bragg gratings were adopted to improve the device integrality without using external circulators [19]. To improve the SMSR by suppressing spurious mode coupling, a two-stage tilted Bragg grating was employed [20]. In this work, the performance of the tunable filter element is improved further for the purpose of demonstrating an integrated tunable transceiver. Air trenches and lower electrodes are introduced to extend the wavelength-tuning range to 40 nm, and a polymer with very low birefringence is adopted to resolve the polarization dependence [21]. In addition, by reducing the insertion loss of the device to less than 3 dB and implementing SMSR exceeding 40 dB, performance levels suitable for 5G fronthaul optical communication networks are demonstrated.

## 2. DESIGN OF TUNABLE TRANSCEIVERS CONSISTING OF TUNABLE LASERS AND TUNABLE FILTERS

Based on the polymer waveguide Bragg-grating technology, a compact integrated tunable transceiver is proposed as shown in Fig. 1. The tunable laser consists of a superluminescent diode (SLD) gain chip attached to the end of a polymer waveguide and a Bragg grating at the other end, which constitute an external cavity laser (ECL). The output wavelength is tunable by heating the electrode under the Bragg grating. Besides, the tunable wavelength filter has two stages of inclined Bragg gratings and asymmetric Y branches for mode sorting. When the WDM signal arrives at the receiver, it passes through the mode-sorting Y branch consisting of narrow and wide waveguides, and a mode evolution occurs to produce an odd mode in the

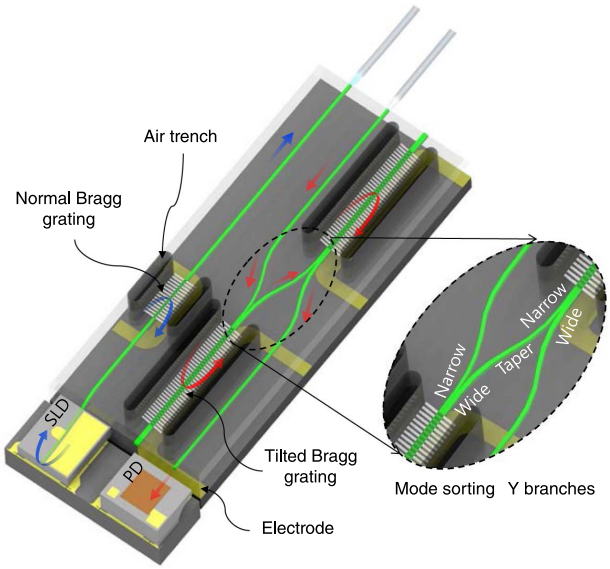


**Fig. 1.** Schematic diagram of the tunable transceiver consisting of a tunable laser and tunable wavelength filter based on polymer waveguide Bragg reflectors. The tunable laser consists of an SLD gain chip attached at the end of the polymer waveguide with a Bragg grating at the other end. The tunable wavelength filter has two stages: an inclined Bragg grating as well as the mode-sorting Y branches.

tilted grating region. By the Bragg reflection by tilted grating, the odd mode is converted to the even mode. The reflected even mode, when it returns to the Y branch, evolves into the wide waveguide. This series of mode-conversion processes can be referred to as a narrow-odd-even-wide (NOEW) mode conversion. When a spurious mode coupling occurs in the asymmetric Y-branch, an undesired reflection occurs through a narrow-even-even-wide (NEEW) mode conversion, which deteriorates the SMSR [22]. The light reflected from the first-stage device enters the narrow waveguide of the second-stage asymmetric Y-branch waveguide through the waveguide taper. After passing through the NOEW mode-conversion process once again in the second-stage device, the filtered signal is detected by the photodetector.

To find the single-mode waveguide condition, effective index of the guided mode is calculated as a function of waveguide width as shown in Fig. 2(a). A perfluorinated polymer (LFR series) produced by ChemOptics Co. is used for device fabrication, and the refractive indices of the materials of the core and cladding layers are 1.396 and 1.371, respectively, for the wavelength of 1550 nm. Given a core thickness of 2.5 μm, the single-mode condition is satisfied for a waveguide width less than 4 μm, and the width of the two-mode waveguide for the tilted grating is determined to be 7 μm.

Bragg gratings for tunable laser are designed using a transmission matrix method. To fabricate the first-order grating with a period of approximately 0.5 μm, laser interferometry is required. However, for the integration of the laser and filter elements on a single chip, as targeted in this work, Bragg gratings of different structures must be created simultaneously using conventional photolithography. Therefore, a fifth-order Bragg grating is adopted for the integration purpose. Given a waveguide width of 3.5 μm, a core thickness variation between 2.5 and 3.2 μm in the Bragg grating produces a reflectivity of 23% for a grating length of 1 mm. The free spectral range of the external cavity laser becomes 0.11 nm for the waveguide length of 0.4 and 0.66 mm in the SLD and Bragg grating, respectively.

The mode coupling efficiency of the tilted Bragg grating used in the tunable filter is calculated using the mode overlap integral [19,23]. The odd- and even-mode profiles of the two-mode waveguide with a width of 7 μm are calculated, and then the coupling efficiencies between the odd–even modes $\eta_{oe}$, odd–odd modes $\eta_{oo}$, and even–even modes $\eta_{ee}$, are obtained as a function of tilt angle $\theta_t$, respectively, as shown in Fig. 2(b). At $\theta_t$ of 3°, $\eta_{oe}$ became the maximum while $\eta_{oo}$ the minimum, which implies that the odd mode was completely converted to the even mode. The tilted grating had a period of 2.81 μm, and the modulation depth of grating was the same as that of the tunable laser, 0.7 μm. For single and double reflections, the reflectance and 20 dB bandwidth for $\eta_{oe}$, depending on the grating length, are calculated as shown in Fig. 2(c). For a grating length of 6 mm, the reflectance due to double reflection is calculated to be 89.3%, and the return loss is 0.49 dB. The reflectance is slightly lower than that of the single reflection, but the bandwidth is much narrower. For a grating length 6 mm, 20 dB bandwidth and reflectance are examined as functions of the effective index difference $\Delta N_{eff}$ due to the grating

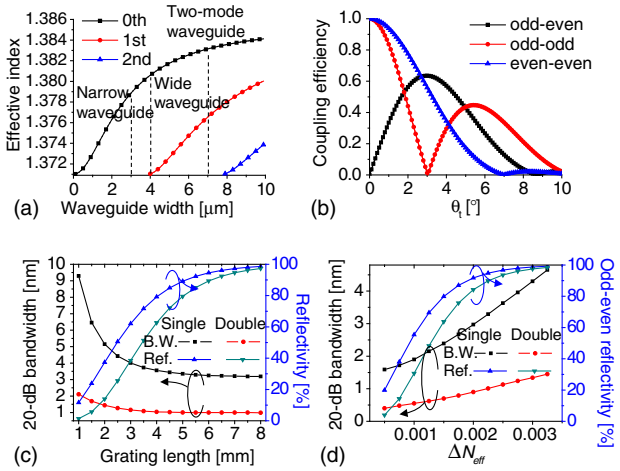


**Fig. 2.** Design results of the proposed device. (a) The effective index of the guided mode is calculated according to the waveguide width to find the single-mode and two-mode conditions. (b) Coupling efficiencies calculated as functions of the tilt angles between the odd–even modes $\eta_{oe}$, odd–odd modes $\eta_{oo}$, and even–even modes $\eta_{ee}$. (c) Reflectivity and 20 dB bandwidth for odd–even coupling along the grating length, compared for single and double reflections. (d) 20 dB bandwidth and reflectance calculated as functions of the effective index difference $\Delta N_{\text{eff}}$ due to the Bragg-grating thickness modulation.

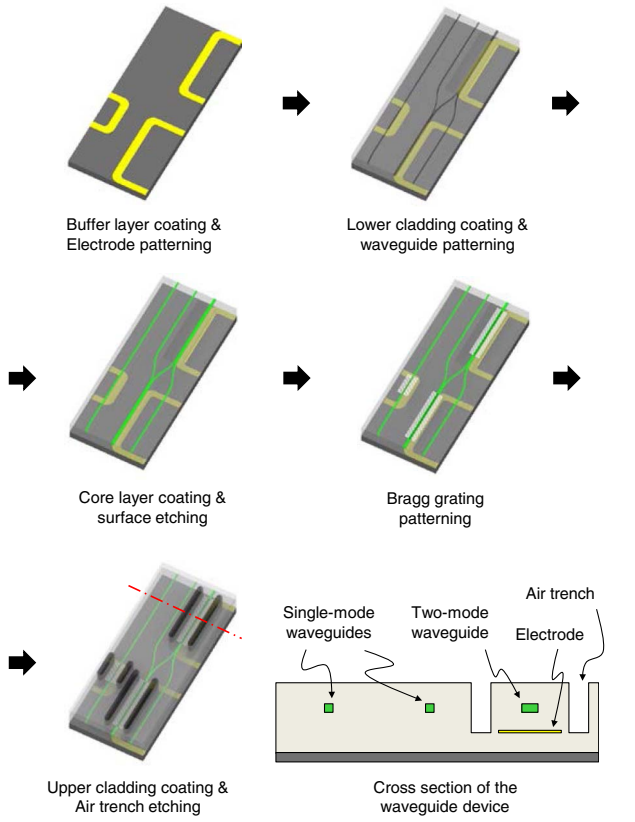


**Fig. 3.** Schematic of the fabrication procedure of the proposed two-stage connected wavelength-tunable filter and tunable wavelength laser. The two devices can be fabricated using the same fabrication procedure. The device cross section is shown along the red dashed single dotted line.

thickness modulation as shown in Fig. 2(d). As $\Delta N_{\text{eff}}$ increases, the 20 dB bandwidth increases significantly in the case of single reflection and is maintained in the case of double reflection.

To consider the modal crosstalk in the asymmetric Y-branch waveguide, the adiabatic mode evolution process is simulated using the beam-propagation method. For a branch with an angle of 0.3° and narrow and wide waveguide widths of 3 and 4 μm, respectively, we find that the crosstalk can be less than −30 dB. As the angle increases, the crosstalk increases because of the higher-order mode scattering.

In order to expand the wavelength-tuning range, it is necessary to prevent the radiation of the guided mode caused by the thermal gradient. The heater located above the waveguide creates a temperature gradient in the core of the optical waveguide, creating a vertical gradient of refractive index profile. In particular, the odd mode existing in the two-mode waveguide is severely affected by the index gradient, resulting in large waveguide loss [20]. To overcome this problem and increase the tuning range, we minimize the thermal gradient by adopting a bottom electrode and introducing an air trench structure on the sides of the heater [24,25].

## 3. FABRICATION OF TUNABLE LASERS AND TUNABLE FILTERS BASED ON POLYMER BRAGG GRATINGS

Because the fabrication procedure of the tunable laser is similar to that of the tunable filter, this paper focuses on the fabrication process of the tunable filter, which is shown by a schematic diagram in Fig. 3. Self-assembled metal nanoparticles are formed on the surface of a silicon substrate, and $CF_4$ plasma dry etching is performed to increase the adhesion of the polymer thin films on Si wafer. After coating a 9 μm thick buffer layer on the silicon substrate, an electrode pattern is formed with AZ5214 photoresist. Cr-NiCr-Au of 80-100-3500 Å (1 Å = 0.1 nm) is sputtered, and the photoresist is lifted off. Then, LFR polymer with a refractive index of 1.371 is coated as a lower cladding layer of 13 μm thickness. To produce an optical waveguide pattern, a 50 Å thick Cr layer is sputtered, an AZ5206 photoresist pattern is defined, and Cr is wet-etched. The waveguide pattern is transferred to the lower cladding layer through oxygen plasma etching. The etching depth is 4.7 μm, and the widths of the asymmetric Y-branches are measured as shown in Fig. 4(a), which is close to the design target ($W_n = 3$ μm, $W_w = 4$ μm, $W_w = 7$ μm). LFR polymer with a refractive index of 1.396 is coated to a thickness of 6 μm to fill the grooves formed in the cladding, and the entire surface is etched to remain a core thickness of 3.1 μm.

To fabricate the fifth-order Bragg grating, 50 Å thick Au layer is deposited through sputtering and a Bragg-grating pattern is formed through contact photolithography using diluted AZ5206. The Bragg-grating pattern is transferred to the core layer through oxygen plasma etching. Figure 4(b) shows the scanning electron microscope (SEM) photograph of the Bragg grating formed with a modulation depth of 0.7 μm and a period of 2.8 μm. The upper cladding is formed with

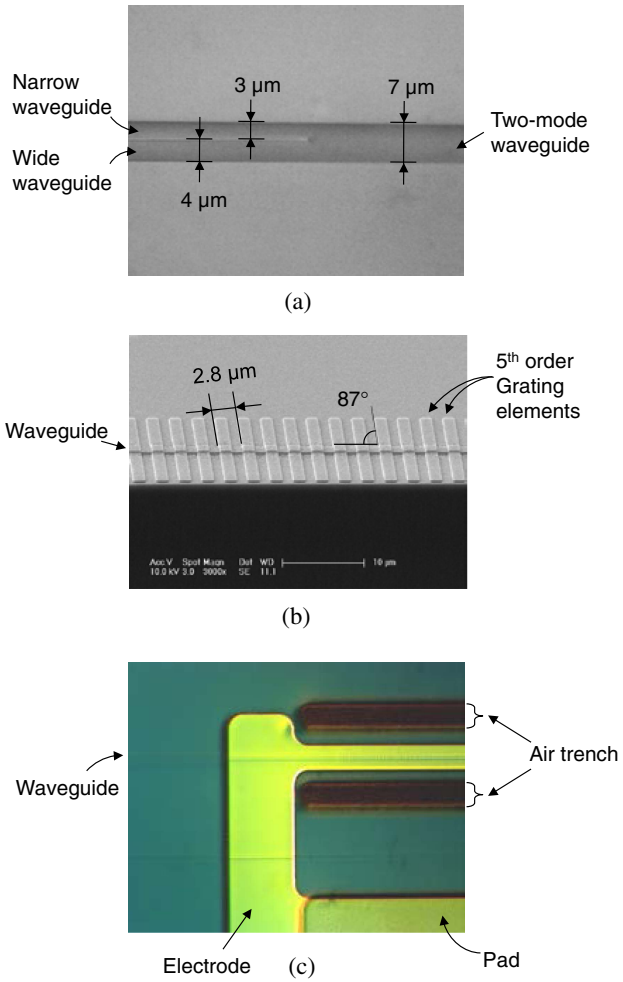


**Fig. 4.** (a) Microscopic photograph of optical waveguide pattern in the asymmetric Y-branch region, where 3, 4, and 7 mm waveguides are defined by etching through the Cr metal mask. (b) SEM photograph of fifth-order Bragg-grating pattern fabricated on top of the waveguide core through contact photolithography. (c) Microscopic photograph of air trenches and electrode pad opened by using the oxygen plasma etching.

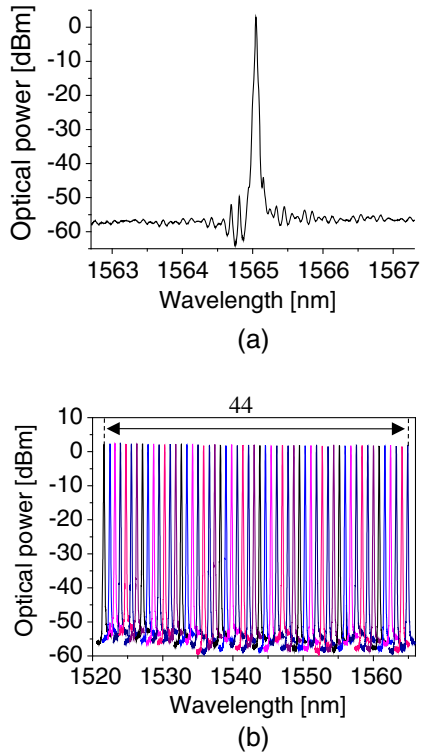


**Fig. 5.** (a) Tunable laser output spectrum measured with an OSA when 50 mA current was applied and (b) lasing spectra measured step by step while gradually increasing the power applied to the Bragg-grating electrode, in which the wavelength-tuning efficiency was 0.207 nm/mW and the power fluctuation was less than 1 dB.

the same polymer as the lower cladding, and the total thickness of the polymer layer becomes 31 μm. After depositing Cr of 100 nm thickness, an air trench and an electrode pad are opened by plasma etching using AZ5214 photoresist as shown in Fig. 4(c). End-facet polishing is carried out with sandpapers starting from coarse to fine grit size, and optical-grade polishing is completed using diamond suspensions. After finishing the end-facet polishing, an SLD is butt-coupled to the chip to form the ECL.

## 4. MEASUREMENT OF POLYMER WAVEGUIDE DEVICE CHARACTERISTICS

The SLD used for the tunable wavelength laser had a center wavelength of 1540 nm, 3 dB bandwidth of 40 nm, and threshold current of 30 mA. For an applied current of 50 mA, CW laser spectrum was measured with an optical spectrum analyzer (OSA) as shown in Fig. 5(a). The output wavelength was determined by the reflection wavelength of the polymer Bragg grating as 1565 nm. To confirm the wavelength tuning, the lasing spectrum was measured step by step with gradual increase of the applied power on the grating electrode. As shown in Fig. 5(b), the spectra for 55-channel output signal wavelengths were produced at a channel spacing of 100 GHz, the wavelength-tuning efficiency was 0.207 nm/mW, and the laser output fluctuation was observed to be less than 1 dB over the entire range. The SLD gain chip was attached on the edge of polymer waveguide chip, and the coupling loss was less than 3 dB.

In order to characterize the tunable filter, an SLD with a 3 dB bandwidth of 100 nm and center wavelength of 1558 nm was aligned to the wavelength filter through a fiber with high numerical aperture (NA). A fiber-optic polarization controller was used to adjust TE-polarized light, and then the light was sequentially reflected from the two Bragg gratings before it was measured using the OSA. The device initially exhibited a large loss and an abnormally narrow bandwidth because of the slightly different reflection spectra between the two Bragg gratings, affected by the fabrication uniformity. To match the reflection spectra, an additional bias power was applied to one of the Bragg gratings, and as a result a reflection spectrum with an SMSR of 36 dB and insertion loss of 3.17 dB was obtained as shown in Fig. 6(a). The bandwidths of 0.5, 3.0, and 20 dB were observed to be as narrow as 0.2, 0.38, and 0.67 nm,

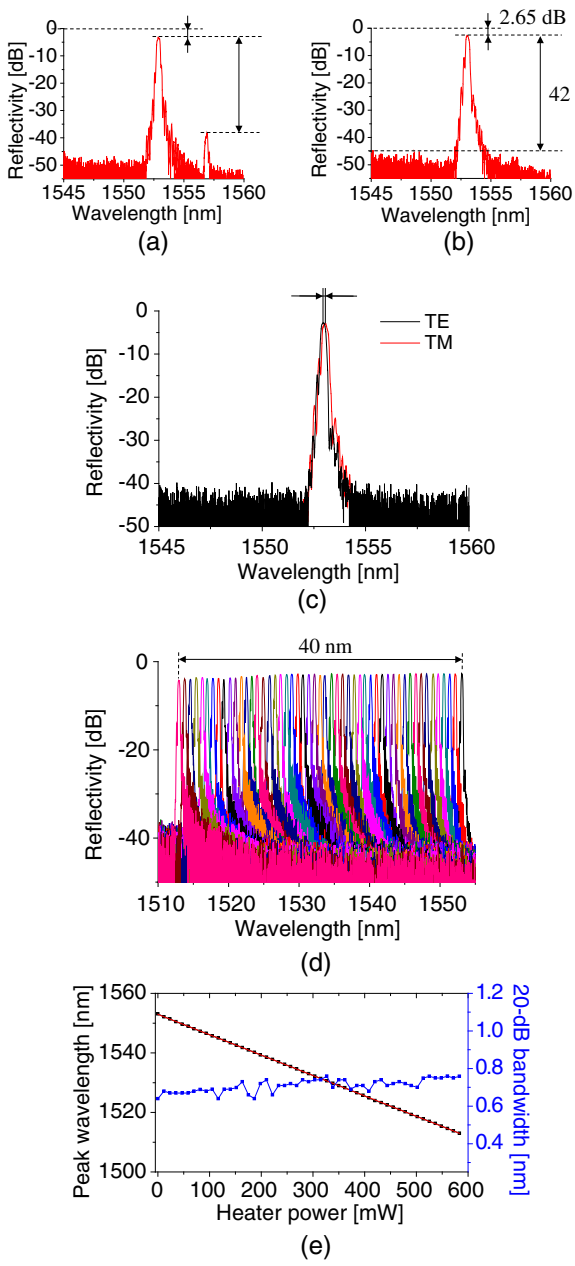


**Fig. 6.** (a) Reflection spectrum of the double-reflection tunable wavelength filters after the adjustment of two slightly different reflection spectra by applying a bias voltage when the two gratings have slightly different properties. (b) Reflection spectrum of another device with improved fabrication uniformity where the two Bragg gratings have identical reflection spectrum. (c) Polarization dependence of the reflection spectrum for the TE and TM modes, where only 0.08 nm of polarization dependence was observed. (d) Reflection spectra measured by increasing the heating power in steps. (e) Wavelength change drawn with respect to the input power, where linear wavelength tuning was achieved with a wavelength-tuning efficiency of 68.5 nm/W and 20 dB bandwidth was maintained below 0.8 nm.

respectively. Since the uniformity in the fabrication process was improved to have the same reflection peaks from the two tilted Bragg gratings, a clean reflection spectrum was obtained without applying the bias as shown in Fig. 6(b). Moreover, the device exhibited a high SMSR exceeding 40 dB and a low insertion loss of 2.6 dB owing to the suppressed NEEW reflection.

High-NA fiber with a core diameter of 1.8 μm and NA of 0.350 was used to reduce the coupling loss between the optical fiber and the polymer waveguide. The coupling loss between the high-NA fiber and the single-mode fiber could be as low as 0.1 dB by performing an adequate splicing process producing a tapered fiber core. Through the cutback method, the propagation loss of the polymer waveguide was measured to be 0.32 dB/cm for the wavelength of 1550 nm. Then the tunable filter with a length of 3.6 cm was expected to have a propagation loss of 1.15 dB, and the coupling loss to the high-NA fiber was measured to be 0.35 dB/facet. The loss due to the two Bragg gratings was expected to be 0.5 dB, and the excess loss by the asymmetric Y branch was 0.3 dB. By controlling the input polarization with a fiber-optic polarization controller, the polarization dependence of reflection peak was measured to be 0.08 nm and the polarization dependent insertion loss was 0.3 dB as shown in Fig. 6(c).

Wavelength-tuning characteristics were measured by increasing the heating power in steps. As shown in Fig. 6(d), 50 channels were produced at 100 GHz channel spacing. The insertion loss variation over the entire tuning range was maintained below 1.5 dB, and the SMSR was above 25 dB. The wavelength change with respect to the input power was measured as shown in Fig. 6(e). Linear wavelength tuning was achieved with a tuning efficiency of 68.5 nm/W, and the 20 dB bandwidth was maintained below 0.8 nm.

## 5. CONCLUSION

Based on the unique characteristics of the polymer waveguide tunable Bragg grating, we demonstrated tunable lasers and tunable filters that could be integrated into a single chip. The external cavity tunable laser consisting of polymer Bragg grating and SLD exhibited an output power of 4.2 dBm and allowed 55 wavelength channels at a spacing of 100 GHz. The tunable filter consisting of a tilted Bragg grating and an asymmetric Y branch was designed in a two-stage cascaded structure to achieve narrow reflection bandwidth, high SMSR, and low adjacent-channel crosstalk. In particular, the introduction of an air trench and a bottom-electrode structure solved the problem of radiation in the two-mode optical waveguide, which was an obstacle to widening the wavelength-tuning range. In addition, by introducing perfluorinated LFR polymer with low birefringence, polarization independence, an essential condition for a wavelength filter device, was secured. The tunable filter exhibited a 20 dB bandwidth of 0.69 nm, wavelength-tuning range of 40 nm, and SMSR of 42 dB, and it satisfied all the specifications required for 5G WDM fronthaul application. It is the first demonstration toward monolithic single-chip tunable transceiver modules based on polymeric tunable Bragg gratings, and these devices would be highly useful for data-center communication networks.

**Funding.** National Research Foundation of Korea (2020R1A2C2101562).

**Acknowledgment.** This research was supported by a National Research Foundation of Korea (NRF) grant funded by the Korean government (MSIP).

**Disclosures.** The authors declare no conflicts of interest.

## REFERENCES

1. M. J. Marcus, "5G and 'IMT for 2020 and beyond' [spectrum policy and regulatory issues]," IEEE Wireless Commun. **22**, 2–3 (2015).
2. T. Pfeiffer, "Next generation mobile fronthaul and midhaul architectures," J. Opt. Commun. Netw. **7**, B38–B45 (2015).
3. B. Skubic, G. Bottari, P. Öhlén, and F. Cavaliere, "The role of DWDM for 5G transport," in *European Conference on Optical Communication* (IEEE, 2014), pp. 1–3.
4. Y.-O. Noh, H.-J. Lee, J. J. Ju, M.-S. Kim, S. H. Oh, and M.-C. Oh, "Continuously tunable compact lasers based on thermo-optic polymer waveguides with Bragg gratings," Opt. Express **16**, 18194–18201 (2008).
5. S.-H. Oh, K.-H. Yoon, K.-S. Kim, J. Kim, O. Kwon, D.-K. Oh, Y.-O. Noh, J.-K. Seo, and H.-J. Lee, "Tunable external cavity laser by hybrid integration of a superluminescent diode and a polymer Bragg reflector," IEEE J. Sel. Top. Quantum Electron. **17**, 1534–1541 (2011).
6. G. Jeong, J.-H. Lee, M.-Y. Park, C.-Y. Kim, S.-H. Cho, W. Lee, and B.-Y. Kim, "Over 26-nm wavelength tunable external cavity laser based on polymer waveguide platforms for WDM access networks," IEEE Photon. Technol. Lett. **18**, 2102–2104 (2006).
7. D. de Felipe, Z. Zhang, W. Brinker, M. Kleinert, A. Maese Novo, C. Zawadzki, M. Moehrle, and N. Keil, "Polymer-based external cavity lasers: tuning efficiency, reliability, and polarization diversity," IEEE Photon. Technol. Lett. **26**, 1391–1394 (2014).
8. A. Malik, J. Guo, M. A. Tran, G. Kurczveil, D. Liang, and J. E. Bowers, "Widely tunable, heterogeneously integrated quantum-dot O-band lasers on silicon," Photon. Res. **8**, 1551–1557 (2020).
9. J. Minowa and Y. Fujii, "Dielectric multilayer thin-film filters for WDM transmission systems," J. Lightwave Technol. **1**, 116–121 (1983).
10. Y. Hibino, "Recent advances in high-density and large-scale AWG multi/demultiplexers with higher index-contrast silica-based PLCs," IEEE J. Sel. Top. Quantum Electron. **8**, 1090–1101 (2002).
11. T. Inui, T. Komukai, and M. Nakazawa, "Highly efficient tunable fiber Bragg grating filters using multilayer piezoelectric transducers," Opt. Commun. **190**, 1–4 (2001).
12. A. Sneh and K. M. Johnson, "High-speed continuously tunable liquid crystal filter for WDM networks," J. Lightwave Technol. **14**, 1067–1080 (1996).
13. P. Tayebati, P. D. Wang, D. Vakhshoori, and R. N. Sacks, "Widely tunable Fabry-Perot filter using Ga(Al)As-$AlO_x$ deformable mirrors," IEEE Photon. Technol. Lett. **10**, 394–396 (1998).
14. F. Ye, H.-S. Lee, and R. Schleicher, "Compact high-resolution tunable optical filter using optical diffraction element and a mirror," U.S. patent 7,899,330 (March 1, 2011).
15. T. Nakazawa, S. Taniguchi, and M. Seino, "Ti:$LiNbO_3$ acousto-optic tunable filter (AOTF)," Fujitsu Sci. Tech. J. **35**, 107–112 (1999).
16. J. R. Ong, R. Kumar, and S. Mookherjea, "Ultra-high-contrast and tunable-bandwidth filter using cascaded high-order silicon microring filters," IEEE Photon. Technol. Lett. **25**, 1543–1546 (2013).
17. M.-C. Oh, W.-S. Chu, J.-S. Shin, J.-W. Kim, K.-J. Kim, J.-K. Seo, H.-K. Lee, Y.-O. Noh, and H.-J. Lee, "Polymeric optical waveguide devices exploiting special properties of polymer materials," Opt. Commun. **362**, 3–12 (2016).
18. G. Huang, J.-S. Shin, W.-J. Lee, T.-H. Park, W.-S. Chu, and M.-C. Oh, "Surface relief apodized grating tunable filters produced by using a shadow mask," Opt. Express **23**, 21090–21096 (2015).
19. T.-H. Park, J.-S. Shin, G. Huang, W.-S. Chu, and M.-C. Oh, "Tunable channel drop filters consisting of a tilted Bragg grating and a mode sorting polymer waveguide," Opt. Express **24**, 5709–5714 (2016).
20. T.-H. Park, S.-M. Kim, and M.-C. Oh, "Polymeric tunable wavelength filter with two-stage cascaded tilted Bragg gratings," Opt. Express **28**, 10145–10152 (2020).
21. S.-H. Park, J.-K. Seo, J.-O. Park, H.-K. Lee, J.-S. Shin, and M.-C. Oh, "Transmission type tunable wavelength filters based on polymer waveguide Bragg reflectors," Opt. Commun. **362**, 96–100 (2016).
22. T.-H. Park, G. Huang, E.-T. Kim, and M.-C. Oh, "Optimization of tilted Bragg grating tunable filters based on polymeric optical waveguides," Curr. Opt. Photon. **1**, 95–100 (2017).
23. J. M. Castro, D. F. Geraghty, S. Honkanen, C. M. Greiner, D. Iazikov, and T. W. Mossberg, "Optical add-drop multiplexers based on the antisymmetric waveguide Bragg grating," Appl. Opt. **45**, 1236–1243 (2006).
24. T.-H. Park, S.-M. Kim, S.-H. Park, J.-K. Seo, H.-G. Lee, and M.-C. Oh, "Polymer waveguide WDM channel selector operating over the entire C and L bands," Opt. Express **26**, 16323–16332 (2018).
25. Z. Zhang and N. Keil, "Thermo-optic devices on polymer platform," Opt. Commun. **362**, 101–114 (2016).